

# The wire array Z-pinch programme at Imperial College

M. G. Haines 1), S. V. Lebedev 1), J. P. Chittenden 1), S.N. Bland 1), F.N.Beg 1), A. E. Dangor 1), S.A.Pikuz 2), T.A.Shelkovenko 2)

1) The Blackett Laboratory, Imperial College, London SW7 2BZ, U. K.

2) P.N.Lebedev Physics Institute RAS, Moscow, 117924, Russia

**Abstract.** Plasma formation and implosion dynamics of wire array z-pinchs have been studied experimentally using the MAGPIE generator (1.4MA, 240ns) at Imperial College. Simulations and theory verify much of the data. Both laser probing and x-ray radiography show after an initial volumetric heating of the wires the presence of dense wire cores surrounded by low density coronal plasma. Radiography shows development of perturbations on the dense core of each wire, while laser probing shows inward jetting of the coronal plasma caused by the global  $\mathbf{J}\times\mathbf{B}$  force, and these plasma streams are axially non-uniform on the same spatial scale as later seen in the wire cores. The spatial scale of these perturbations ( $\sim 0.5\text{mm}$  for Al,  $\sim 0.25\text{mm}$  for W) increases with the size of the wire cores ( $\sim 0.25\text{mm}$  for Al,  $\sim 0.1\text{mm}$  for W). The inward flow of the coronal plasma is usually field free and leads to formation on the array axis of a straight plasma column, the dynamics of which is strongly affected by radiation cooling. Images obtained by optical streak camera show that the wire cores start their inward motion late and the implosion trajectory deviates significantly from the expected from 0-D analysis. An increase of the number of wires (decrease of inter-wire gap) resulted in a transition to 0-D trajectory for aluminium wire arrays, but not for tungsten. In experiments with nested wire arrays two modes of behaviour are observed; in the first the inner array is transparent to the imploding outer array, but the current transfers to it, leading to a fast implosion. The second mode occurs when a significant fraction of current is flowing in the inner array and the two arrays apparently implode simultaneously. In both modes the x-ray pulse is significantly sharpened in comparison with that generated in implosion of a single wire array.

## 1. Introduction

Recent Z-pinch experiments utilising cylindrical arrangements of fine metallic wires as loads have produced record X-ray powers and efficiencies [1,2]. This has sparked great interest in the ICF community who hope to use the X-rays to energise hohlraums for indirect drive fusion research [3]. It is thought that the power and the rise-time of the generated X-ray pulses are primarily determined by the development of the Rayleigh-Taylor (R-T) instability in the imploding plasma. There is a general understanding that the higher the number of wires in the array, the more symmetric the load and the higher the resultant X-ray power – indicating a reduction in the level of R-T, but the development of the instability is not fully understood.

Plasma formation in a wire array and indeed in a single wire is heterogeneous. At the start of the current pulse, there is a ‘dwell time’ during which very little expansion of plasma is seen around the wires. Once this dwell time has elapsed material starts to rapidly ablate from each wire to form a ‘core-corona’ system [4]: a cold, dense, relatively unionised wire ‘core’ continually ablates forming a surrounding hot, low density ‘coronal’ plasma. Initially the cores appear stationary and the  $\mathbf{J}\times\mathbf{B}$  force of the global magnetic field accelerates coronal plasma from around each core into streams that flow towards the array axis. When the coronal streams stagnate on axis, a column of precursor plasma is produced [5,6]. The process of core ablation and coronal plasma streaming continues until cores start to accelerate and this is accompanied by the development of a global R-T instability. Once the cores reach the axis, the array ‘stagnates’ and an X-ray pulse is emitted.

In this paper we present studies of the core-corona system in wire arrays, detailing the development of instabilities in the corona and how these instabilities can be transferred to the

cores to seed the global R-T instability. We show how the implosion trajectory of the cores undergoes change with wire number. Finally, the use of 2 concentric arrays, the ‘nested configuration’, is examined as a way of reducing R-T.

## 2. Plasma Formation and The Precursor

Experiments were performed on the MAGPIE generator [7] with current rising to 1MA in 240ns. Arrays were of 16mm diameter and 2.3cm long with 8, 16, 32 or 64 wires (usually 15  $\mu\text{m}$  Al or 4 $\mu\text{m}$  W). The diagnostic set-up included laser probing, a soft X-ray gated camera, a radial optical streak camera and diamond photo-conducting detectors (PCDs), and is described elsewhere [6]. To enable examination of the wire cores, an X-ray backlighting system (imaging flash photography with X-rays) has been developed (fig 1). Two or four crossed wires are placed in one of MAGPIE’s current return posts forming an ‘X-pinch’ [8]. As current flowed through the X-pinch, the cross over point collapses, producing a short duration (<1ns) point source of hard X-rays. A camera on the other side of the array records the image. The timing of the pulse was adjusted by using different diameters of wires in the X-pinch, whilst the probing energy was restricted to 3-5KeV by a titanium filter placed before the film.

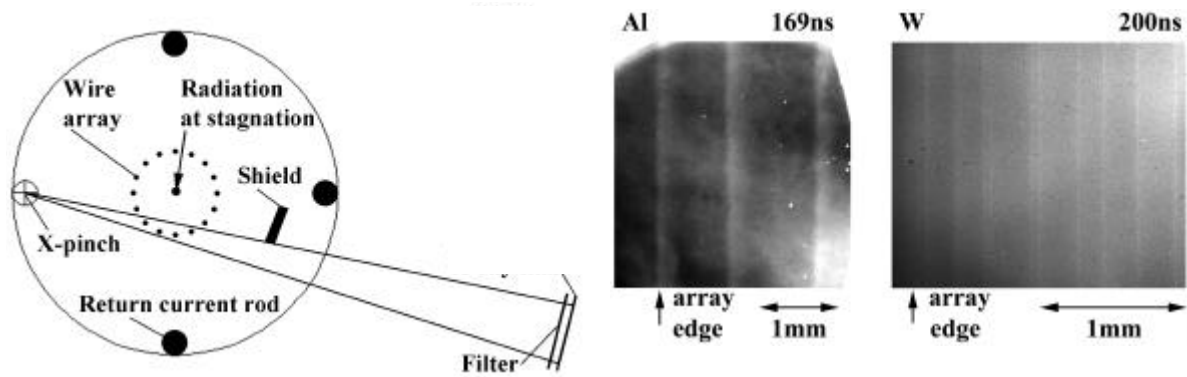


FIG. 1. X-ray backlighting set-up

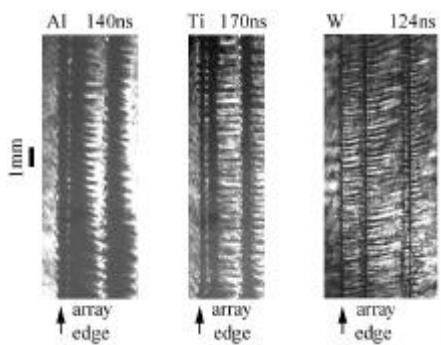


FIG. 2. Side-on schlieren photo of edge wires in Al, Ti and W wire arrays array.

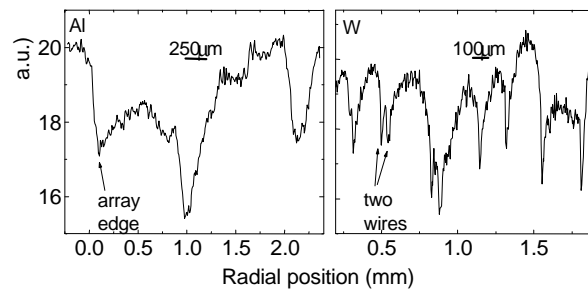


FIG. 3. X-ray backlighting images of Al and W arrays and corresponding film densities.

Laser probing data shows that after  $\sim 60\text{ns}$ , low density coronal plasma from the wires starts streaming towards the array’s axis, forming a narrow precursor plasma column at about half the implosion time. The streaming is accompanied by the development of instabilities as seen on schlieren and shadow images (e.g. Fig. 2). Coronal plasma from each wire within the array seems to demonstrate the same instability wavelength, but the instability is uncorrelated between wires. The wavelength of instability appears unaffected by initial wire diameter and current per wire, but does depend on material: aluminium displays a characteristic wavelength

of  $\lambda \sim 0.5\text{mm}$ , whilst tungsten has  $\lambda \sim 0.25\text{mm}$ . The large extent of the instability structure in the inward radial direction ( $\delta R \sim 5-10\lambda$ ) indicates the streams are force-free in nature i.e. no further acceleration occurs as they flow towards the axis. This implies that the magnetic Reynolds' number in the jetting coronal plasma is less than unity. An analytic simplified model of the 3-D unstable and jetting plasma has been developed. In the neck regions where the Joule heating is strong the core is ionised and ablated through flux limited heat flow. This plasma flows to the jets, the radially inward motion being caused by the global magnetic field; the model automatically yields a magnetic Reynolds' number of less than unity.

Fig 3 shows typical X-ray backlighting images of wire cores at the array edge at  $\sim 70\%$  of the implosion time. The cores are still in their original positions. The characteristic sizes of the wire cores are  $\sim 0.25\text{mm}$  for aluminium and  $\sim 0.1\text{mm}$  for tungsten. These sizes are again found to be independent of initial wire diameter and current per wire. There appears to be a dependence of the coronal instability on the core size. Calculating  $ka = (2\pi/\lambda)a$ , where  $\lambda$  is taken from the laser probing and  $a$  is half of the core size measured by backlighting, produces  $ka \sim 1.5$  for both aluminium and tungsten. This implies that the size of the region ( $\sim$ the core size), where the formation and acceleration of the coronal plasma takes place, determines the development of the instability. A similar scaling of wavelength with plasma radius occurs for a single wire, but in contrast the current carrying plasma region is expanding in time. There is very good agreement between the experimental observations and 2-D MHD simulations of

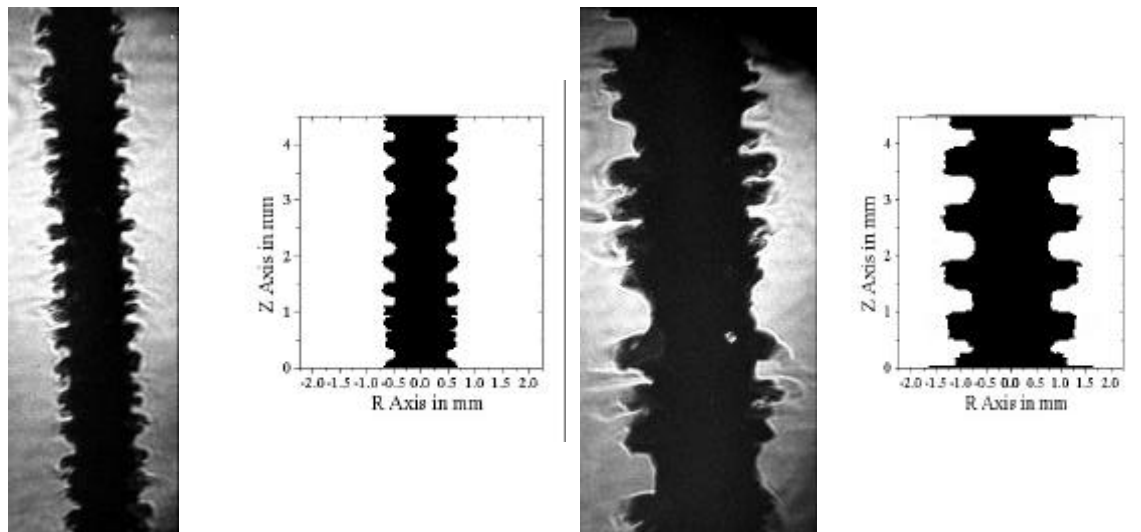


FIG 4. Experimental and simulated laser schlieren images for a  $100\ \mu\text{m}$  aluminum wire on the Cornell generator at 51ns and 85ns.

this system. Fig.4 shows experimental data from a single Al wire compared with a snapshot in the r-z plane from the simulation [9].

### 3.Seeding Of the Rayleigh-Taylor Instability

The coronal instability imprints a mass perturbation on the wire core from which it ablated. Once the cores start to accelerate (see later) these perturbations act as a seed for the development of R-T instability. Backlighting images taken at  $\sim 80\%$  of the implosion time (e.g. Fig. 5) clearly show the outer boundary of the cores having the characteristic bubble and spike structure of the R-T instability. The wavelength of the instability is the same as that of the coronal stream ( $\sim 0.5\text{mm}$  for the aluminium array in figure 2) and, like the stream, is uncorrelated between cores.

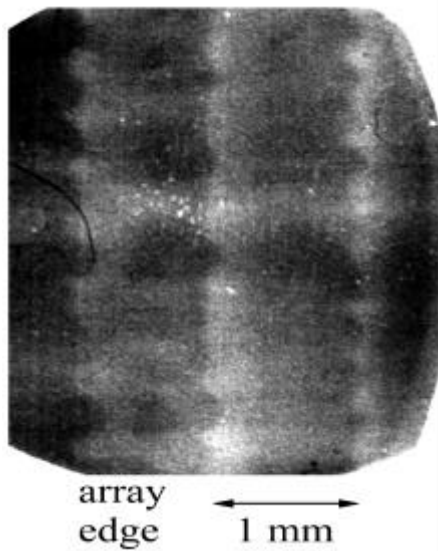


FIG. 5. Backlighting image of Al array showing R-T in individual cores of wires.

Perturbations in the individual cores can act as a seed towards the global, correlated, R-T instability that develops shortly after they start to accelerate. However, the global instability has a longer wavelength than that in individual cores (e.g. an aluminium array produces a global R-T of  $\lambda \sim 2\text{mm}$  [6]). The precise mechanism that determines the global wavelength requires further investigation, but is possibly related to the fact that for a longer wavelength mode the effect of the perturbations in individual cores being out of phase is smaller. Some evidence of the preferential development of a longer wavelength is seen in Fig 4, where the amplitude of perturbations is larger if they coincide with perturbations in neighbouring cores.

#### 4. Implosion Trajectories

The implosion dynamics of wire cores were measured by radial optical streak photography. The trajectories found were compared to a 0-D model, which assumes that the array implodes as a hollow plasma cylinder accelerated by the global  $\mathbf{J} \times \mathbf{B}$  force.

The implosion trajectories of 8, 16 and 32 aluminium wires and 16, 32 and 64 tungsten wires (Fig. 6) did not agree with the 0-D model. Instead the cores remained in their initial positions until about 80% of implosion time -the time when the imprint of instabilities on wire cores was detected. The stationary

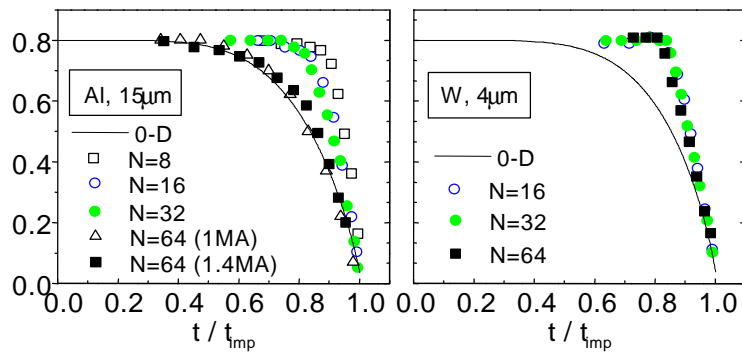


FIG. 6. Core implosion trajectories in  $15\mu\text{m}$  Al and  $4\mu\text{m}$  W arrays.

position of the cores can only be understood if no force is applied to them i.e. until this time the current flows mainly in the coronal plasma just around the cores. The sudden acceleration of the cores would then occur at a time when current transferred to them, probably due to the cores being unable to sustain their rate of mass ablation into the coronal plasma. Assuming that all the current is transferred at  $\sim 80\%$  of implosion time, a mass fraction of  $\sim 25\text{-}50\%$  remaining in the cores would provide the observed fast implosion. The dynamics of array implosion was also studied via computer simulations (in  $r\text{-}\theta$  plane) and Fig.7 shows the inward streaming of the coronal plasma from the wire cores.

In experiments, a qualitative change in the implosion dynamics was observed (Fig. 6) in aluminium arrays when the wire number was increased from 32 to 64 (inter-wire gap decreased from  $1.57\text{mm}$  to  $0.78\text{mm}$ ). The 64 wire trajectory now follows the 0-D model's more closely. A decrease in emission from the precursor was also observed, becoming effectively zero long before stagnation of the array (emission from the precursor in other

arrays continued throughout the implosion). This indicates a possible cut off in mass injection towards the axis.

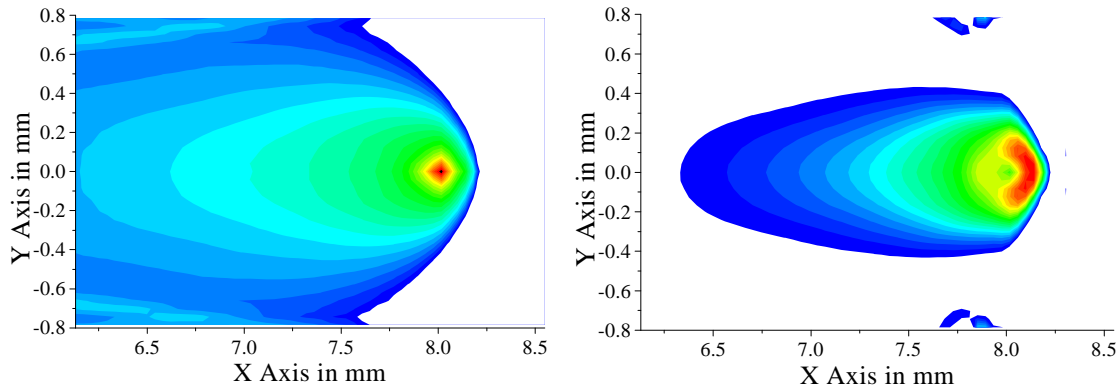


FIG 7. Results of computer modelling of 32 aluminium wire array on MAGPIE generator showing density (left) and current (right) distributions in  $x$ - $y$  plane at  $t = 120$  ns after the current start.

The observed change in the implosion dynamics for aluminium arrays occurred when the ratio between inter-wire separation (0.78mm) and the characteristic size of wire core (0.25mm) became equal to about 3. This could be related to the fact that when the ratio of the inter-wire separation to the wire diameter equals  $\pi$ , the contribution of the ‘private’ magnetic flux of each wire to the array inductance is zero, and the array inductance becomes equal to that of a thin shell. For tungsten wire arrays, which have a core size a factor of  $\sim 2.5$  smaller, this could not occur until the inter-wire gap reached  $\sim 0.3$ mm (which would make the number of wires prohibitively large).

## 5. Different Modes of Nested Wire Array Implosions

‘Nested’ arrays (two concentric arrays, one inside another) have been utilised at Sandia National Labs and led to a 40% increase in X-ray power over single arrays [10]. Three different ‘modes’ of interaction between the arrays have been suggested (fig 8). The first, ‘hydrodynamic collision’ mode, assumes that both outer and inner arrays form annular shells.

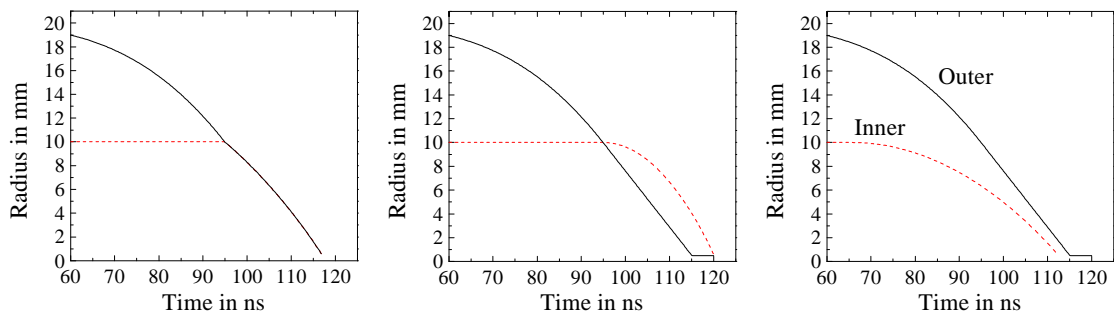


FIG. 8. 3 modes of nested implosion: a) hydrodynamic collision b) transparent inner c) magnetic buffer.

The outer accelerates, and when it hits the inner, the R-T instability is reduced. The combined plasma then implodes too rapidly for any further R-T to grow to excessive levels. The second, ‘transparent inner’ mode [11], assumes that the inner array is shielded from current by the outer and remains as discrete wires. Plasma from the outer array passes straight through the gaps in the inner array. The current then switches to the inner array and the resulting plasma implodes rapidly onto the outer material that has already reached the axis. The inner implodes

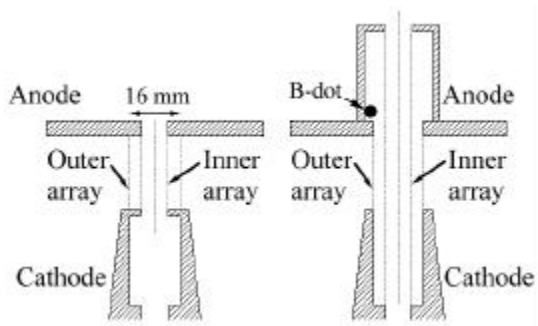


FIG 9. Schematic of nested wire arrays with (left) low inductance and (right) high inductance connection of the inner array.

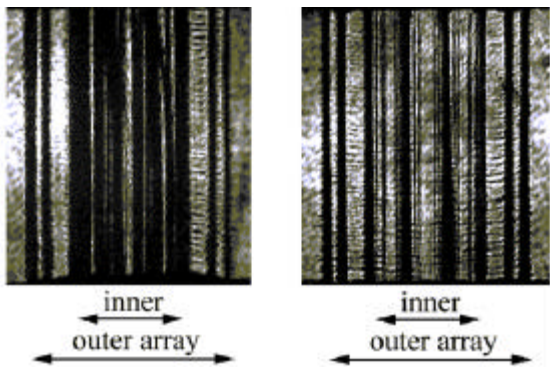


FIG. 10. Shadowgrams of a normal array (left) and the high-L array (right) at 128ns and 134ns.

so quickly that again the R-T does not have time to grow to an excessive level. The third, 'magnetic buffer' mode, assumes that some flux is trapped between the arrays and compressed as the outer starts to move. The compressed flux drives in the inner array, and the result is that the outer and inner never collide but, instead, can reach the axis simultaneously.

It is likely that all 3 processes occur in nested configurations, but one process dominates according to the current flowing through and the number of wires in the inner array [12]. A high number of wires or their expansion by current leads to a high degree of momentum transfer from the outer to the inner and a mostly hydrodynamic collision. A low number of wires with little current flowing through them produces an implosion dominated by current transfer.

Our experiments [13] with nested wire arrays on MAGPIE has concentrated on isolating the transparent inner mode. To achieve this, a special nested array, the 'high-L' array, has been developed (Fig 9). The outer array is identical to the single 16 wire 15 $\mu$ m aluminium arrays

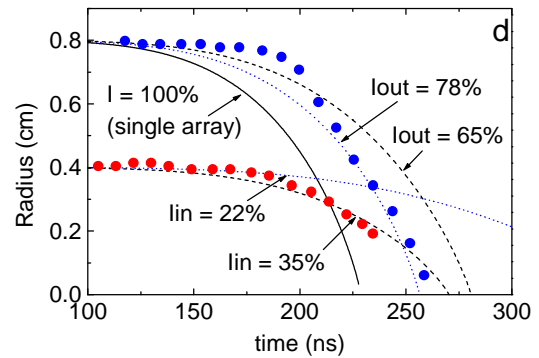
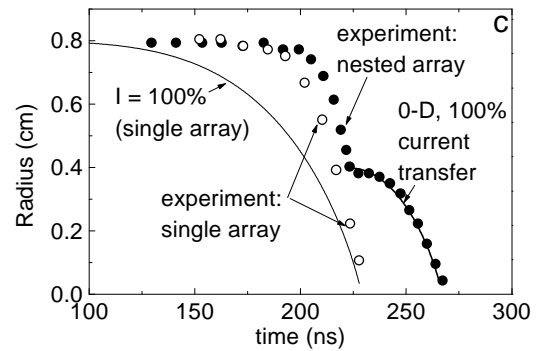
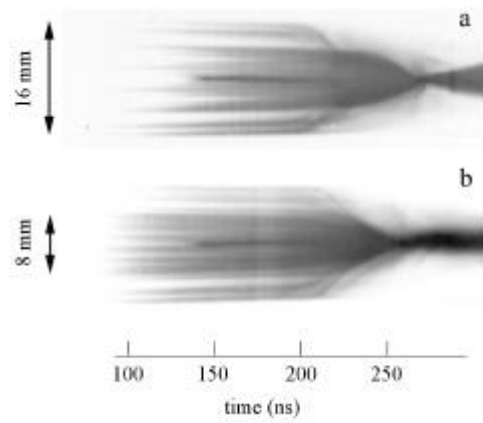


FIG. 11. Radial optical streak photographs and comparison of the inferred radial positions of the inner and outer arrays with the 0-D model for high inductance (a,c) and low inductance (b,d) arrays.



used in the previous experiments. The inner array was half the diameter of the outer, again used 16 wires of 15 $\mu$ m aluminium, but was  $\sim 3$  x the length, increasing its inductance and limiting the current flowing through it. To illustrate the difference in current flow, Fig 10 shows two shadowgrams taken at the same time - one from a normal nested array, the other from the high L one. No measurable expansion is seen from the inner wires of the high-L.

Radial optical streaks were used to study the array dynamics (Fig.11). The trajectory of the outer array was much the same as that of a single 16 wire array, with the cores remaining at the initial radius until  $\sim 80\%$  of a single array implosion time and only then accelerating the inwards. The inner array in high-L case remained stationary before the outer passed by, and immediately afterwards its velocity was still zero – indicating no momentum transfer from the outer to the inner. The inner array then started to accelerate towards the axis and its implosion trajectory closely follow the 0-D model, assuming that all the current was flowing through the central 2.3cm section.

Very different implosion dynamics are observed for nested arrays with low inductance connection of the inner array. The radial position of the outer array (Fig.11b,d) after  $\sim 220$ ns follows quite closely a 0-D trajectory with 78% of the current in the outer array (the fraction of current expected from the mutual inductance of the arrays). The inner array starts to move

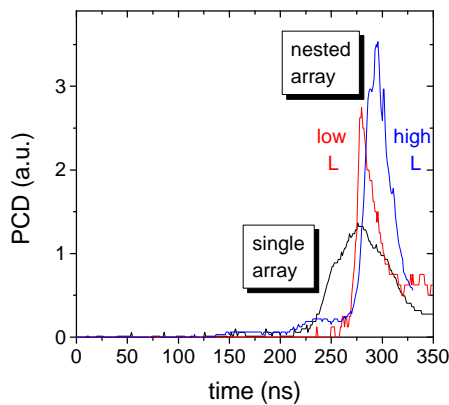


FIG. 12. Soft x-ray signals from single and nested wire arrays.

at  $\sim 175$ ns and initially follows the 0-D trajectory for the remaining 22% of current, but later, from  $\sim 200$ ns, the inner array implodes faster and the closest 0-D trajectory corresponds to  $\sim 35\%$  of the current. As a result the two arrays apparently stagnate simultaneously and no collision of the arrays is observed in this case.

The time history of soft x-ray emission recorded by a PCD detector with a 5 $\mu$ m polycarbonate filter (transmission window 180 - 290eV) is shown in Fig.12. In all cases the main x-ray pulse starts at the time of stagnation, measured from the streak images. For a single array the pulse rise-time (10-90%) is 40ns. Nested wire arrays (in both configurations) produce x-ray pulses with much shorter rise-times of 10 - 13ns, despite the long implosion times (260 - 270ns) and small numbers of wires. The mechanism of x-ray pulse shortening is probably different for the two configurations. For the low L case the magnetic field between the arrays could affect the growth of the R-T instability, but more data are needed here. In the high L case almost the maximum current is rapidly applied to the inner array and the R-T instabilities in the inner array have less time to grow (smaller  $\int \gamma dt$ ) due to a short implosion time. It is interesting to note that the shape of the x-ray pulse (“foot” before the main pulse) for the high inductance case is very similar to that observed in nested array implosions on the Z facility (see Fig.2 in Ref. [10]), despite a very large difference in the number of wires in the arrays (240 in outer and 120 in inner in Ref. [10] and 16/16 in our experiments).

## 6. Conclusion

Considerable progress has been made in the understanding of the physics of wire array implosions. The plasma formed from each wire of the array has a core-corona structure and MHD instabilities develop on each wire from early time. Previous work [14,6] showed that these early instabilities are uncorrelated and the later global  $m=0$  mode of Rayleigh-Taylor instability was shown to be seeded by these individual instabilities with  $N^{-1/2}$  perturbation amplitude scaling consistent with the heuristic model [14]. In the present paper we have shown that the dense wire cores survive for a substantial part of the implosion, and for inter-wire separation above some critical value, the cores remain in the initial positions of wires until  $\sim 80\%$  of the implosion time. It was found that for Al wire arrays the decrease of the inter-wire separation to 0.8mm resulted in a qualitative change in the implosion dynamics and transition to the 0-D trajectory. The critical inter-wire gap appears to be related to the size of dense wire cores, measured in our experiment by x-ray radiography, and the transition to 0-D-like implosion occurred when the ratio between the gap and the core size became equal to  $\sim 3$ . For tungsten the core size is significantly smaller ( $\sim 0.1$ mm instead of  $\sim 0.25$ mm for Al), which explains the absence of transition to a 0-D implosion trajectory in our experiments, and suggests that a similar deviation of the implosion from a shell-like probably occurs in tungsten wire array experiments at SNL even for large wire number arrays. The experiments with nested wire arrays show that significant sharpening of the x-ray pulse can be obtained in different modes of interaction between the outer and inner arrays, and even for arrays with small wire numbers. For the mode with a transparent inner wire array, the outer array passes through the inner, which then implodes due to the fast transfer of current from the outer array at this time, as was theoretically predicted by J. Davis et al [11]. The almost maximum current is rapidly applied to the inner array in this case, and the R-T instability has much less time to grow. In addition, it is possible that the level of perturbations in the inner array, which initially does not carry current, is smaller in this mode. The existence of different implosion modes of nested wire arrays, all giving a sharper x-ray pulse, will allow pulse shaping, a necessary requirement for optimising capsule implosion in indirect drive IFE.

This work was supported by Sandia National Laboratories (contract BF6405), by AWE through the William Penney fellowship and by U.S. Department of Energy (Contract No. DE-FG03-98DP00217).

## References

- 1 SANFORD T.W.L. et al., Phys. Rev. Lett. **77**, 5063 (1996).
- 2 DEENEY C. et al., Phys. Rev. **E 56**, 5945 (1997).
- 3 MATZEN M.K., Phys. Plasmas **4**, 1519 (1997).
- 4 LEBEDEV S.V. et al., Phys. Rev. Lett, **85**, 98 (2000).
- 5 AIVAZOV I.K. et al., Sov. J. Plasma Phys. **14**, 110 (1988).
- 6 LEBEDEV S.V. et al., Phys. Plasmas **6**, 2016 (1999).
- 7 MITCHELL I.H. et al., Rev. Sci. Instr. **67**, 1533 (1996).
- 8 SHELKOVENKO T.A. et al, Rev. Sci. Instrum **70**, 667 (1999).
- 9 CHITTENDEN J.P. et al., Phys. Rev. E **61**, 4370 (2000).
- 10 DEENEY C. et al., Phys. Rev. Lett. **81**, 4883 (1998).
- 11 DAVIS J. et al, Appl. Phys. Lett. **70**, 170 (1997).
- 12 CHITTENDEN J.P. et al., Phys. Rev. Lett, submitted.
- 13 LEBEDEV S.V. et al., Phys. Rev. Lett. **84**, 1708 (2000).
- 14 HAINES M.G., IEEE Trans. Plasma Sci. **26**, 1275 (1998).